Protein Expression and Purification 172 (2020) 105630

Contents lists available at ScienceDirect

Protein Expression and Purification

journal homepage: www.elsevier.com/locate/yprep

Cloning, expression and purification of the low-complexity region of RanBP9 protein

Shailendra Dhakal, Krishna Sapkota, Faqing Huang, Vijayaraghavan Rangachari*

Department of Chemistry and Biochemistry, School of Mathematics and Natural Sciences, University of Southern Mississippi, Hattiesburg, MS, 39406, United States

ARTICLE INFO

Keywords:
In vivo cloning
Recombinant expression
Fusion protein
Low complexity region
RanBP9
Disordered protein
Neurodegenerative disease

ABSTRACT

Recombinant expression and purification of proteins is key for biochemical and biophysical investigations. Although this has become a routine and standard procedure for many proteins, intrinsically disordered ones and those with low complexity sequences pose difficulties. Proteins containing low complexity regions (LCRs) are increasingly becoming significant for their roles in both normal and pathological processes. Here, we report cloning, expression and purification of *N*-terminal LCR of RanBP9 protein (Nt-RanBP9). RanBP9 is a scaffolding protein present in both cytoplasm and nucleus that is implicated in many cellular processes. Nt-RanBP9 is a poorly understood region of the protein perhaps due to difficulties posed by the LCR. Indeed, conventional methods presented difficulties in Nt-RanBP9 cloning due to its high GC content resulting in insignificant protein expression. These led us to use a different approach of cloning by expressing the protein as a fusion construct containing mCherry or mEGFP using *in vivo* DNA recombination methods. Our results indicate that expression of mEGFP-tagged Nt-RanBP9 followed by thrombin cleavage of the tag was the most effective method to obtain the protein with > 90% purity and good yields. We report and discuss the challenges in obtaining the *N*-terminal region of RanBP9, a protein with functional implications in multiple biological processes and neurodegenerative diseases.

1. Introduction

Low-complexity regions (LCRs) of a protein are sequences containing statistical enrichment of a small sub-set of amino acid types in comparison to random sequences. Human genome contains at least 10% of encoded proteins as LCRs [1], which are increasingly recognized as key modulators of protein functions. Many LCRs are capable of undergoing liquid-liquid phase separation (LLPS) and organizing into membraneless organelles [2]. Many proteins containing prion-like low-complexity domains are also known to aggregate into cross-β sheet fibrils that are often linked to pathological effects [3]. LCRs are more commonly observed to be disordered, although some folded proteins also possess such regions [4]. Needless to say, the increased importance of LCRs warrants deeper investigations into proteins containing such regions.

Ran binding protein 9 (RanBP9) is an evolutionarily conserved protein that is present predominantly in brain, heart and skeletal muscles. It localizes both in nucleus and cytoplasm and is known to play many important cellular processes such as apoptosis, cell adhesion, migration, transcription, and has been hypothesized to be a scaffolding protein [5]. The protein is also involved in pathological roles in Alzheimer disease (AD), Schizophrenia and cancer [6–8]. Recent studies have established the interaction of RanBP9 with amyloid precursor protein (APP), β-secretase APP cleaving enzyme (BACE1), and low density lipoprotein receptor-related protein (LRP) leading to increased Aβ generation, which is one of the important hallmarks of AD [9]. Similarly, RanBP9 has been shown to restrict several cell signaling pathways to promote tumorigenesis [10]. The 78 kDa RanBP9 protein consists of five conserved domains: a *N*-terminal proline and glutamine-rich domain (RanBP9 1–130 termed, Nt-RanBP9, which is the focus of this work), spore lysis A and ryanodine receptor (SPRY) domain, lissencephaly type-I-like homology (LisH) motif, C-terminal to LisH (CTLH) motif, and C-terminus (CRA) (Fig. 1a) [11]. Although diverse roles mediated by full length RanBP9 as well as those of the domains are known both in norm and pathology, the structure and function of proline and glutamine-rich *N*-terminal domain (1–130) remains to be the least understood region of the protein. Since a nuclear import sequence (NIS) is located on the C-terminal side of this disordered region (140–160), we hypothesize that the *N*-terminal region could be involved in transcriptional regulation [12]. One of the reasons for the paucity of information on the domain could be attributed to its predicted structural disorder [5,13], which renders conventional structural

* Corresponding author.
E-mail address: vijay.rangachari@usm.edu (V. Rangachari).

https://doi.org/10.1016/j.pep.2020.105630
Received 10 March 2020; Received in revised form 19 March 2020; Accepted 19 March 2020
Available online 23 March 2020
1046-5928/

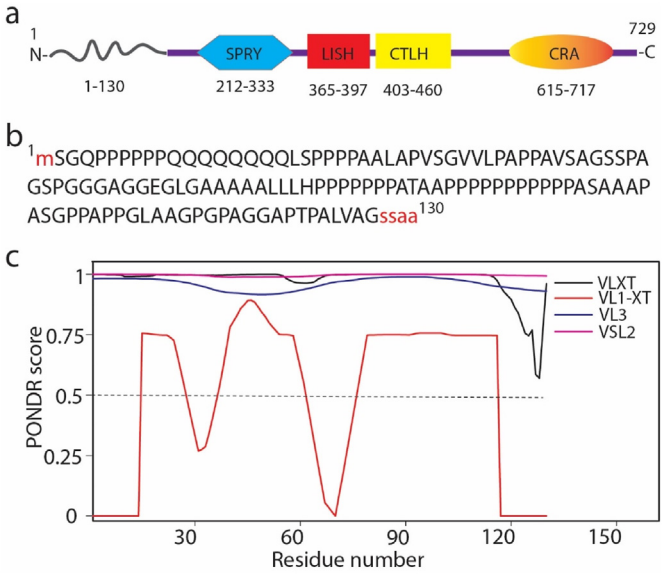

Fig. 1. *In silico* analysis of low complexity disordered region of Nt-RanBP9 a) Schematic of full length RanBP9 protein. b) Results of LCR analysis using SEG algorithm (SEG masker). LCR of Nt-RanBP9 are shown in upper case letters. c) PONDR showing disordered region of Nt-RanBP9. PONDR score reflects protein disorder; any residue with score more than 0.5 is considered to be disordered.

biology tools ineffective. Furthermore, the *N*-terminal sequence seems to be populated with only a few select amino acids, making it an archetypical LCR (elaborated further down in the manuscript). It is known that recombinant expression of LCRs are not trivial and are complicated with difficulties in transcriptional and translational levels, as well as increased post-translational proteolytic cleavage [14]. Since multiple attempts failed to express Nt-RanBP9 from BL21 (DE3) cells containing the expression plasmid pNt-RanBP9 (described further down), we reasoned that the unusual sequences of both within the DNA template (high GC content) and the low complexity protein sequence might negatively impact the early translation stage. Furthermore, the intrinsically disordered Nt-RanBP9 might inhibit its own translation. Therefore, to overcome these difficulties, here we report cloning, expression and purification of Nt-RanBP9 with a modified design and construction of pET-based plasmids containing fluorescent proteins mCherry and mEGFP fused at the *N*-terminus.

2. Materials and methods

2.1. Nt-RanBP9 cloning

Cloning of Nt-RanBP9 into the fluorescent plasmid backbones pmCherry PHisP1 and pmEGFP-PhisP1 was performed with modifications according to our established *in vivo* assembly of PCR-generated DNA fragments with overlapping ends [15]. Instead of using uncut plasmids as the templates for PCR through two consecutive rounds to reduce the background as in the original procedure [15], all template plasmids were thoroughly digested with appropriate restriction enzymes to eliminate uncut plasmid, while keeping the template region intact. When PCR failed to produce the desired DNA fragments, appropriate restriction enzymes were used to generate the DNA fragments from plasmids, followed by agarose gel purification. DNA recovery from cut gel pieces was accomplished by the Zymoclean Gel DNA Recovery Kit (Zymo Research). DNA oligos were obtained from Thermo Fisher Scientific, whose Value Oligos offer a distinct advantage for generating DNA fragments with overlapping ends by PCR. High fidelity Q5 DNA polymerase (New England Biolabs) was used to prepare DNA fragments. For plasmid assembly, agarose gel-verified DNA fragments generated by either PCR or restriction enzymes were mixed at equal volumes (the total volume can be from 1 to 5 μL, and the molar ratio may vary from 1:1 to 1:10). The mixture was then transformed into DH5α competent cells (10–50 μL cells, New England Biolabs). After overnight growth, 2 randomly selected colonies were picked from each plate, followed by plasmid preparation. A panel of restriction enzymes (New England Biolabs) were then used to digest isolated plasmids, followed by agarose gel electrophoresis. Correct plasmid assembly was confirmed by the restriction DNA patterns. Lastly, a single validated plasmid from each *in vivo* cloning was used to transform BL21 (DE3) cells for the purpose of recombinant protein expression and purification. Since the *in vivo* cloning procedure based on the homologous recombination principle is highly precise and accurate [15], sequencing of isolated plasmids is often unnecessary.

2.2. Transformation and expression of Nt-RanBP9 constructs in E. coli

Transformation and expression of protein was carried out using established protocols. Briefly, 10 ng of Nt-RanBP9 with or without mCherry/GFP-tagged plasmids were mixed with 5 μL of ice thawed BL21 (DE3) competent cells (Invitrogen). Mixture was incubated on ice followed by heat shock for 30 s at 42 °C. Then, 100 μL of SOC media was added into the mixture and incubated for 1 h at 37 °C in the incubator shaker. The mixture was then spread evenly into an LB agar plate containing ampicillin (100 μg/mL) and incubated overnight at 37 °C. A few colonies from plates were grown in LB media until the OD_{600} reached 0.6–0.8 absorbance units. At this stage, 1 mL aliquot of uninduced cells from each tube were taken separately into an Eppendorf tube before inducing protein expression with 0.5 mM IPTG. Cells were grown for 4 h, and protein expression in uninduced and induced samples was analyzed using SDS-PAGE gel (Biorad) and western blotting, and those with good expression were banked in glycerol stocks for cryostorage.

2.3. SDS-PAGE and western blotting

Samples during expression check and purification were subjected to SDS-PAGE analysis using Bio-Rad Mini-PROTEAN®, 4–20% precast gel in denaturing conditions. Briefly, 15 μL of sample was mixed with 5 μL of Laemmli SDS sample buffer, heated for 5 min before loading on the gel, and run in 1X Laemmli running buffer at 210 V. After the run, gel was subjected to coomassie blue staining and/or western blot. For western blot, the gel was transferred to nitrocellulose blotting membrane (Amersham Protran premium 0.45 μm) using Pierce power system (Thermo Fisher). Protein transferred membrane was boiled in 1xPBS for 1 min followed by overnight incubation in blocking buffer (5% non-fat dry milk, 0.1% Tween®-20 in 1X PBS). Blot was incubated for 2.5 h in a solution containing anti-hexahistidine monoclonal antibody (Cell Signaling Technology) and HRP-conjugate anti-rabbit secondary antibody. Finally, blots were washed with 1X PBS and imaged using Pierce ECL western blotting substrate (Thermo Scientific) on a GelDoc molecular imager (Bio-Rad).

2.4. RP-HPLC

The thrombin cleaved protein was run through RP-HPLC in ultimate 3000 series (Thermo scientific) with gradient elution using two mobile phases, water (with 0.1% TFA) and acetonitrile (ACN) (with 0.1% TFA). Before every run, HPLC column (Jupiter C18-Phenomenex 250 × 10 mm) was cleaned and equilibrated with using 95% water and 5% ACN. The gradient was standardized based on the obtained peak resolution. Quantification of Nt-RanBP9 was done using bicinchoninic acid (BCA) assay (Pierce® BCA protein assay kit, Thermo Scientific) with the established protocol.

2.5. CD spectroscopy

CD spectra of samples werewith measured in far-UV region on a Jasco J-815 spectropolarimeter (Jasco,MD). Vacufuged HPLC fractions were resuspended in 20 mM Tris buffer pH 7.0 and were monitored in continuous scan mode from 190 to 260 nm in a 0.1 cm path-length quartz cuvette. Three scans of Nt-RanBP9 at concentration of 15 μM was measured, averaged, blank subtracted and plotted using Origin 7.0.

2.6. MALDI-Tof spectrometry

Samples were analyzed in MALDI-ToF by mixing 1 μL of sample in CH_3CN:H_2O:HCOOH in 1:1:0.1 ratio, and was mixed with equal volume of matrix (sinapinic acid) in the sample solvent. The sample was then loaded on to an MSP 96 BC MALDI plate (Bruker Daltonics). The spectra were collected with a laser power maintained at 70%.

3. Results and discussion

3.1. Intrinsic disorder and low complexity of Nt-RanBP9

The *N*-terminal region of RanBP9 (1–130) is hypothesized to be disordered. A glance at the sequence in this region reveals increased presence of a limited number of amino acids, suggesting low complexity within the region. Specifically, four amino acids, glycine, alanine, proline and serine account for almost 80% of the total amino acids in the sequence (Fig. 1b). In order to confirm whether the *N*-terminus contains canonical LCR, the sequence was analyzed with the complexity prediction program called SEG [4]. This analysis indicated that residues 2–126 constituted a prototypical LCR (Fig. 1b). Similarly, to validate the disorder in the region, the sequence was analyzed with the disorder prediction program, PONDR (www.pondr.com). Different computational prediction algorithms including VLXT (*V*ariously characterized *L*ong disordered regions and two trained on *X*-ray characterized *T*erminal disordered regions), VL1-XT [16], VL3 (trained on *V*ariously characterized and *L*ong disordered regions) [17], and VSL2 (trained on *V*ariously characterized *S*hort and *L*ong disordered regions) [18] (Fig. 2c) revealed Nt-RanBP9 to be intrinsically disordered.

3.2. Cloning of mCherry and mEGFP tagged Nt-RanBP9

Historically, recombinant expression in *E. coli* and biochemical studies of LCRs have been hampered largely by their susceptibility to proteolytic cleavage and aggregation [14]. In our study, RanBP9 1–130 gene was first synthesized commercially (GeneScript Inc). Initial attempts to sub-clone Nt-RanBP9 were unsuccessful because of the difficulty in PCR, which was likely due to its high GC content (described further down). In this regard, *in vivo* cloning through *E. coli*'s intrinsic recombination activity is cheap, fast, and accurate [15,19–25]. Simple transformation of up to 4 DNA fragments with varying lengths of overlapping ends into competent *E. coli* cells produces antibiotic-resistant colonies with correctly assembled plasmids with nearly 100% accuracy [15]. We reasoned that by fusing fluorescent labeled proteins such as mCherry and mEGFP as used previously by Kato and co-workers [14], along with *in vivo* cloning, the shortcomings could be overcome. Therefore, mCherry-Nt-RanBP9 fusion protein gene was designed by joining the mCherry DNA fragment from the backbone plasmid pmCherry PHisP1 (generous gift from Prof. McKnight, UTSW) with the synthetic Nt-RanBP9 DNA from pRanBP9 1–130 in the same open reading frame. The junction contains a NdeI restriction enzyme site but another site for NdeI was also observed within the pmCherry PHisP1 vector. To avoid potential complications during plasmid analysis, the NdeI site in pmCherry PHisP1 was removed first to generate pmCherry PHisP1m by *in vivo* cloning using two DNA fragments containing mutated overlapping ends generated by PCR (Scheme 1). As expected, the gel image (Fig. 2a) shows that the resulting pmCherry PHisP1m lost the NdeI site, while other features such as BsaI and MscI sites, fragment sizes, and the total plasmid size remained the same as those of pmCherry PHisP1.

Subsequently, construction of pmCherry-Nt-RanBP9 was attempted by *in vivo* assembly according to our established procedure [15], as shown in Scheme 2. The mCherry backbone fragment included an added thrombin site to facilitate cleavage of the tag, which was then generated without difficulty by PCR using pmCherry PHisP1m as the template and BKf/mChr primer pairs. However, using the plasmid pRanBP9 1–130 as the template and the Rn9f/Rn9r primer pair, multiple attempts were unsuccessful to amplify the Nt-RanBP9 fragment by PCR due to its high GC content (84%) including the primer binding regions at the ends. Different PCR conditions, including varying annealing temperatures and using a high GC enhancer, were unable to produce the desired Nt-RanBP9 DNA fragment.

While the Nt-RanBP9 fragment could not be amplified by PCR, the DNA fragment is flanked by NdeI and BamHI sites at the ends in plasmid pNt-RanBP9. As an alternative approach, we redesigned an *in vivo* DNA assembly strategy to use the PCR-generated DNA backbone fragment and the restriction-produced Nt-RanBP9 fragment according to Scheme 3. The primer BKf contained an 18 nt overlapping region with Nt-RanBP9 fragment, but the primer mChr did not extend into Nt-RanBP9. Following PCR amplification of the backbone fragment by primer pair BKf/mChr, PCR extension using primer pair BKf/mChre created the additional 15 nt overlapping region at the other end. Transformation of the two DNA fragments into DH5α competent cells

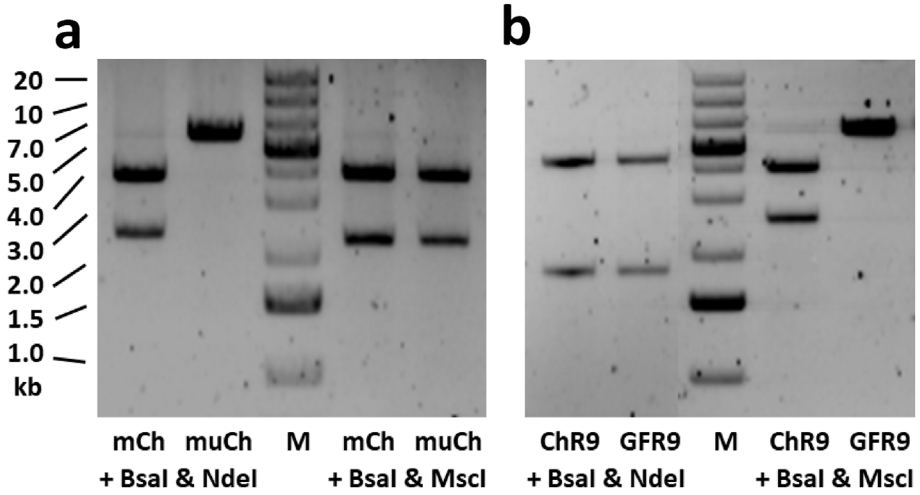

Fig. 2. Confirmation of *in vivo* assembled plasmids by restriction digestion. a) As expected, pmCherry PHisP1 (labeled as mCh) produced 2 bands by BsaI/NdeI digestion (Lane 1, expected 2377 & 3883 bp), and the mutated version pmCherry PHisP1m (labeled as muCh) lacked the NdeI site (Lane 2, 6260 bp). However, both plasmids yielded the same DNA fragments of 2270 & 3990 bp after BsaI/MscI digestion (Lanes 4 & 5). b) pmCherry-Nt-RanBP9 (labeled as ChR9) digestion by BsaI/NdeI (Lane 1, 1856/4687 bp) and BsaI/MscI (Lane 4, 2553/3990 bp) confirms the correct *in vivo* assembly of intended plasmid. Replacement of mCherry with mEGFP produced mEGFP-Nt-RanBP9 (labeled as GFR9), which yielded the expected DNA fragments by restriction digestion, Lane 2 (1856/4696 bp) by BsaI/NdeI and Lane 5 (6552 bp) by BsaI/MscI.

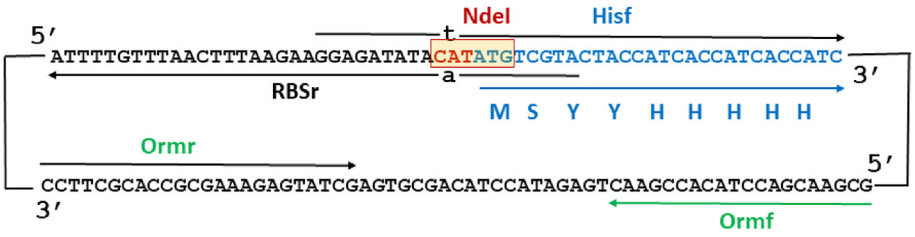

Scheme 1. Removal of the NdeI site in pmCherry PHisP1 by *in vivo* assembly of 2 DNA fragments generated from NdeI-digested pmCherry PHisP1 by PCR with primer pairs HisF/Ormr and Ormf/RBSr, yielding pmCherry PHisP1m. Primers HisF and RBSr contain a mutated basepair ta to disrupt the NdeI site.

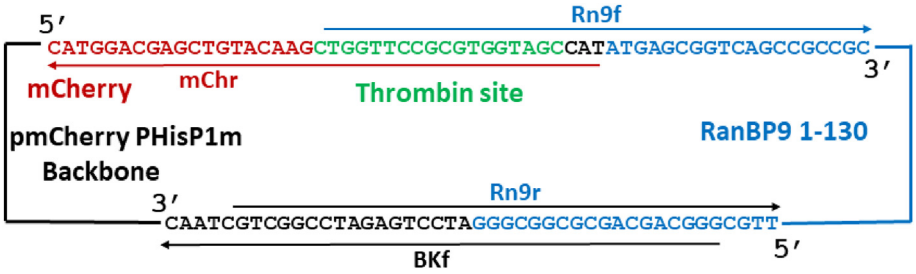

Scheme 2. Design of pmCherry-Nt-RanBP9 construction by *in vivo* assembly of 2 PCR-generated DNA fragments.

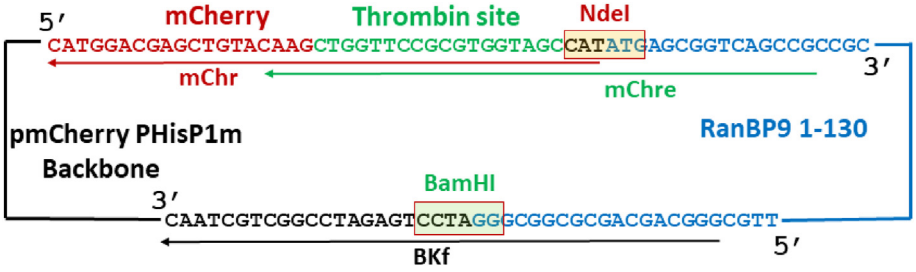

Scheme 3. Alternative design of pmCherry-Nt-RanBP9 construction by *in vivo* assembly of a PCR-generated DNA fragment containing the pmCherry PHisP1m backbone and a BamHI/NdeI-generated Nt-RanBP9 fragment.

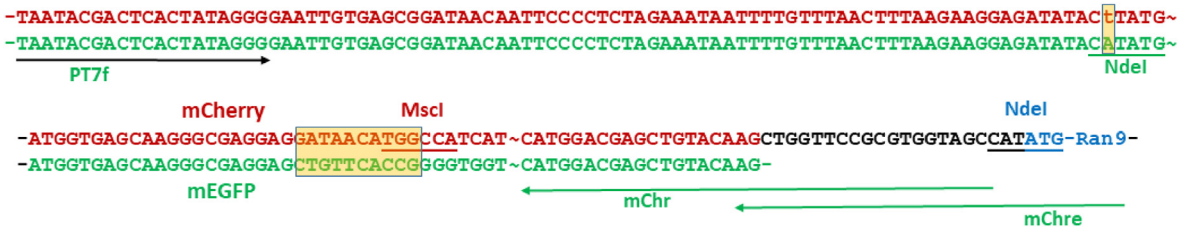

Scheme 4. Design of pmEGFP-Nt-RanBP9 construction by *in vivo* assembly of 2 DNA fragments – the backbone from pmCherry-Nt-RanBP9 digestion by MscI/NdeI and the mEGFP fragment by PCR with PT7f/mchr/mchre. The upper sequence is part of pmCherry-Nt-RanBP9, and the bottom sequence is part of the pmEGFP-PhisP1. The 10 nt mismatch at the pmCherry-Nt-RanBP9's MscI site was corrected during *in vivo* recombination according to the mEGFP sequence. In addition, there was a mismatch at the pmEGFP-PhisP1's NdeI site, which was corrected according to the pmCherry-Nt-RanBP9 sequence.

produced ampicillin-resistant colonies containing the correctly assembled plasmid pmCherry-Nt-RanBP9. As shown in Fig. 2b, digestion of an isolated plasmid by BsaI/NdeI yielded expected 2 bands of 1.9 kb and 4.7 kb (lane 1), while plasmid digestion by BsaI/MscI produced 2 bands of 2.6 kb and 4.0 kb (lane 4), consistent with the predicated 2553 & 3990 bp from the digestion.

Finally, we wanted to construct a different fluorescent protein fusion plasmid pmEGFP-Nt-RanBP9 to remove the impurities that were present in protein purified from pmCherry-Nt-RanBP9 construct. mCherry and mEGFP fragments share a portion of the same sequence at both the 5′ and 3′ ends. In addition, there is an MscI site that is close to the 5′ end of the mCherry fragment. Based on these features, we designed a different *in vivo* cloning strategy (Scheme 4) using the MscI/NdeI-generated backbone from pmCherry-Nt-RanBP9 (top strand) and the PCR-produced mEGFP fragment from pmEGFP-PhisP1 with primers PT7f/mCHr/mChre (bottom strand). Although there were two regions of mismatches (the 1-nt mismatch at the NdeI site in pmEGFP-PhisP1 and the 10-nt mismatch at the McI site in pmCherry-Nt-RanBP9, both boxed), the *in vivo* cloning process repaired both mismatches and yielded correctly assembled plasmid pmEGFP-Nt-RanBP9. As demonstrated in Fig. 2b, digestion of pmEGFP-Nt-RanBP9 by BsaI/NdeI (lane 2) produced the same 2 bands of 1.9 kb and 4.7 kb as generated from pmCherry-Nt-RanBP9 digestion (lane 1), indicating that the boxed NdeI mismatch was repaired to eliminate the NdeI site, while the other NdeI site between mEGFP and Nt-RanBP9 was present. In addition, the MscI site in pmCherry-Nt-RanBP9 (Lane 4) was clearly eliminated during the assembly of pmEGFP-Nt-RanBP9 (Lane 5), resulting in a single band of 6.6 kb by BsaI/MscI digestion (expected 6552 bp).

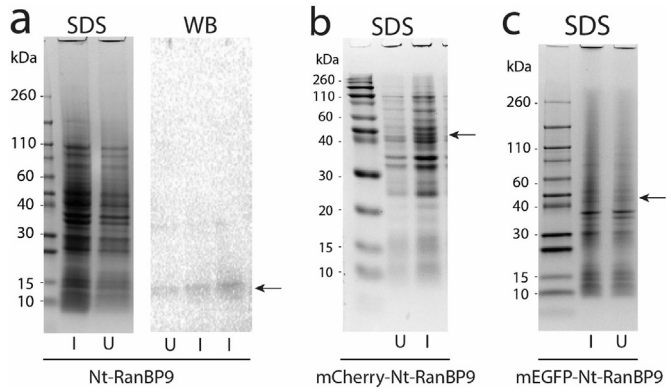

Fig. 3. Expression check of different constructs: a) Nt-RanBP9, b) mCherry-Nt-RanBP9 and c) mEGFP-Nt-RanBP9. SDS and WB indicate coomassie blue stained SDS-PAGE and western blotting with anti-Histidine tag monoclonal antibody; I and U indicated induced and uninduced cells, respectively. Arrows indicate the expected constructs.

3.3. Purification and characterization of Nt-RanBP9 constructs

3.3.1. Nt-RanBP9

First, purification of untagged construct Nt-RanBP9 was attempted without much success (Fig. 3a). When the protein expression in cells was checked by SDS-PAGE followed by coomassie blue staining in un-induced and induced cells, no distinct band corresponding to the protein's molecular weight (~12 kDa) (Fig. 3a) was observed. Hydrophobic and basic amino acid residues are stained more with coomassie blue compared to hydrophilic residues, which are predominant in disordered proteins [26]. This property of IDPs makes it difficult to track the protein expression using coomassie blue or silver staining techniques despite high protein expression. However, protein expression check with western blot using anti-hexahistidine monoclonal antibody showed a faint band of monomeric protein (10–15 kDa) and its dimer (Fig. 3a). This suggests that the protein was either expressed at low levels or getting degraded rapidly, which is a commonly observed issue with proteins containing LCRs.

3.3.2. mCherry-Nt-RanBP9

Due to relatively low protein expression with Nt-RanBP9 protein, expression with mCherry fluorescent fusion tag was attempted to aid in protein expression and purification. Fluorescent tags help in protein expression by increasing solubility and stability of expressed protein

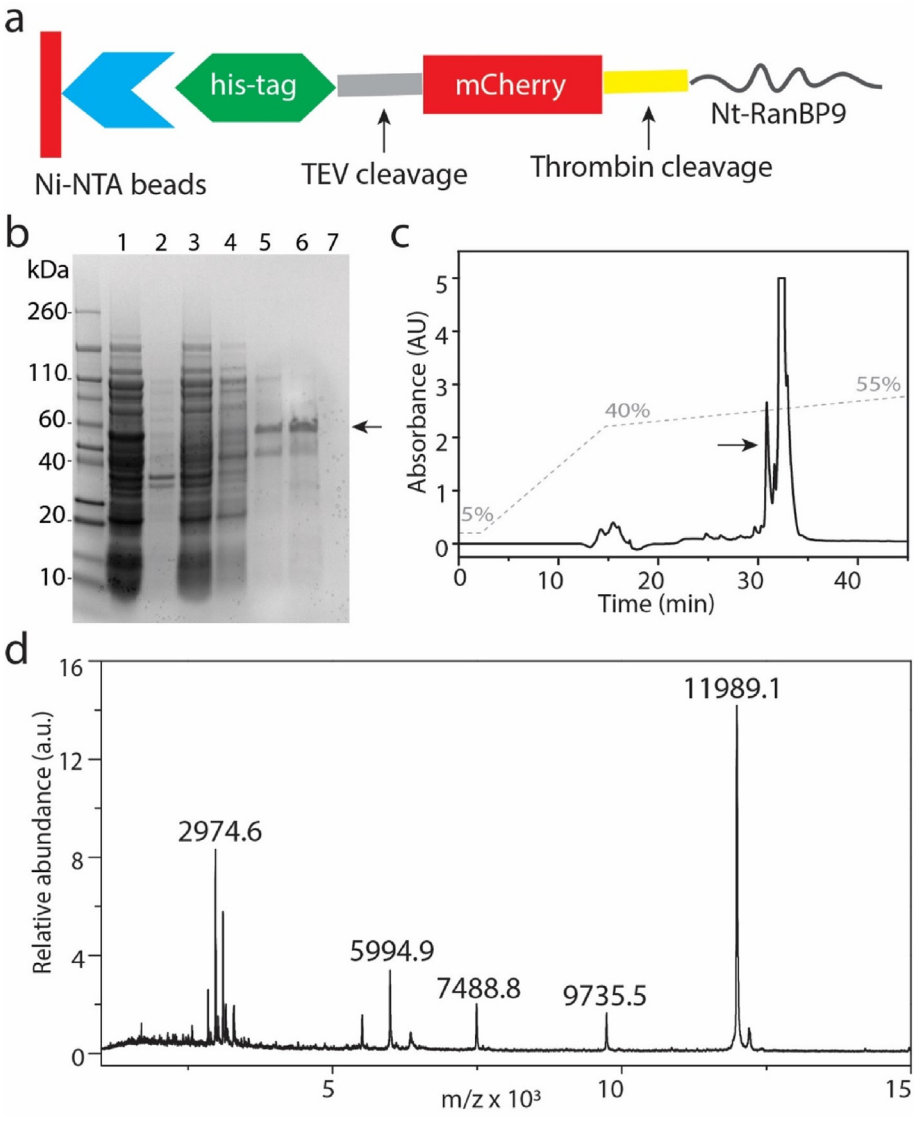

Fig. 4. Purification of Nt-RanBP9 from mcRanBP9 construct. a) Schematic of mCherry-Nt-RanBP9 construct used for purification. b) SDS-PAGE of fractions obtained from Ni-NTA chromatography: supernatant after cell lysis and centrifugation (lane 1), pellet (lane 2), flow through (lane 3), wash with 50 mM imidazole (lane 4), wash with 100 mM imidazole (lane 5), elution with 400 mM imidazole (lane 6), and strip with EDTA (lane 7). c) HPLC purification profile of thrombin cleaved Nt-RanBP9 monitored using UV absorbance at 215 nm. The dotted line shows change in gradient of mobile phase acetonitrile containing 0.1% TFA. d) MALDI-ToF of HPLC fraction containing Nt-RanBP9 (12 kDa), which showed impurities ranging from molecular weight of 2.5 kDa–10 kDa.

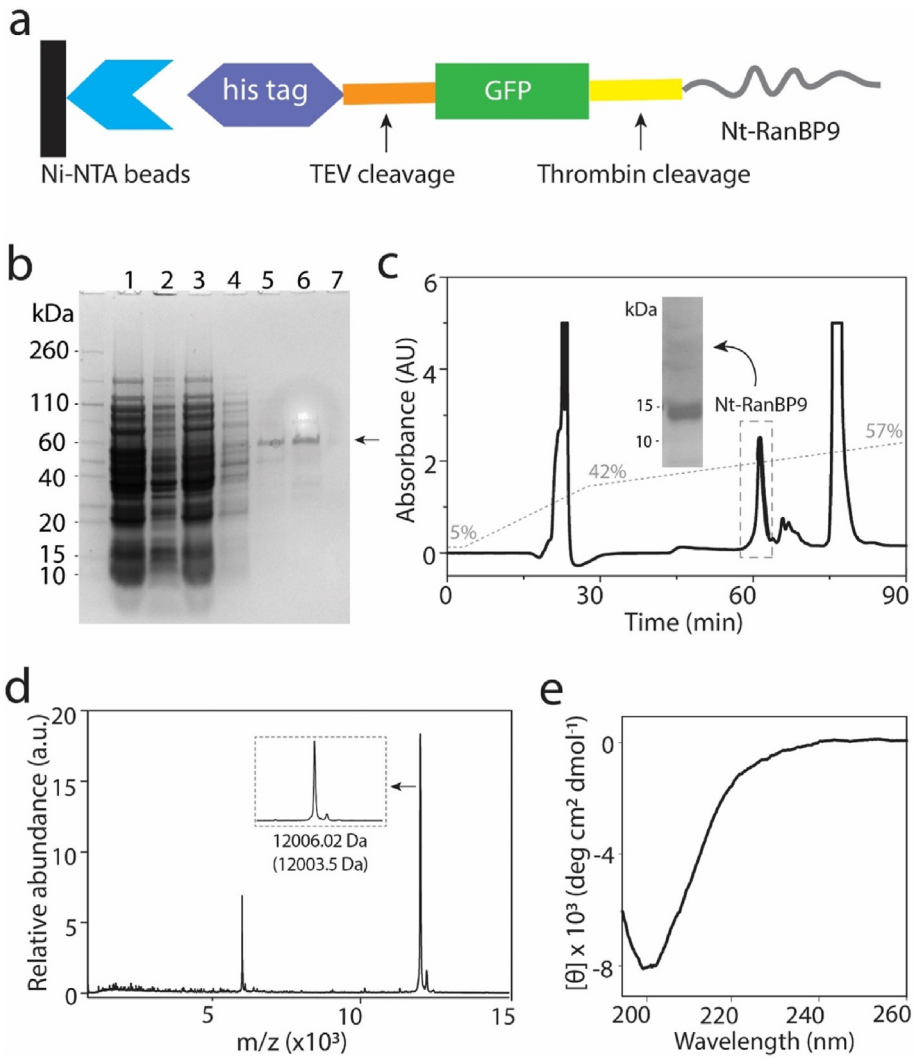

Fig. 5. Purification and characterization of Nt-RanBP9 from gRanBP9 construct a) Schematic of mEGFP-Nt-RanBP9 construct used for purification. b) SDS-PAGE of fractions obtained from Ni-NTA chromatography; supernatant after cell lysis and centrifugation (lane 1), pellet (lane 2), flow through (lane 3), wash with 50 mM imidazole (lane 4), wash with 100 mM imidazole (lane 5), elution with 400 mM imidazole (lane 6), and strip with EDTA (lane 7). c) HPLC purification profile of thrombin cleaved Nt-RanBP9 monitored using UV absorbance at 215 nm along with the confirmation of the protein in SDS-PAGE gel by silver staining (inset). The dotted line shows change in gradient of mobile phase acetonitrile containing 0.1% TFA. d) MALDI-ToF showing protein without impurities. The second abundant peak corresponds to m/2z. e) CD spectra showing random coil with minima around 200 nm.

[27]. Moreover, colorimetric tracking of protein expression and purification process offers advantage to predict amount of expressed protein that eliminates necessity to confirm by other techniques. Coomassie blue staining could not detect the protein as observed with Nt-RanBP9 (Fig. 3b), however, color of cells was visible enough to confirm protein expression. Approximately, 1 g of harvested cells (out of ~3.5 g of cells/L) that expressed fusion protein, mCherry-Nt-RanBP9 with the histidine-tag were resuspended in 10 mL lysis buffer (20 mM Tris, 40 mM NaCl, 10 mM imidazole, 2 M urea, 1 tablet/L equivalent Roche Protease inhibitor cocktail, 1 mM PMSF) maintaining pH 7.0 throughout the experiment. The cells were lysed by sonicating on ice for eight cycles (30 s burst and 1 min rest) followed by centrifugation (9300 × *g* for 10 min). The supernatant thus obtained was subjected to Ni-NTA affinity purification (Fig. 4a). The sample was added to a slurry of Ni-NTA resin (10 mL) pre-equilibrated with lysis buffer in a beaker and incubated in an orbital shaker for 1 h to minimize any protein loss during flow through. The resin was then loaded on to a column and purified in buffer containing 20 mM Tris, 50 mM NaCl, 2 M urea at pH 7.0. The flow-through was collected along with the two washes with buffer containing 50 mM and 100 mM imidazole to remove non-specifically bound proteins. The protein was eluted using elution buffer containing 400 mM imidazole. The column was then stripped with strip buffer (300 mM NaCl, 100 mM EDTA and 20 mM Tris) and stored in 20% ethanol for further use. Aliquots of samples (15 μL) from all these fractions were analyzed using SDS-PAGE that showed an intense band at MW of ~55 kDa corresponding to mCherry-Nt-RanBP9 along with a relatively faint lower molecular weight bands (Fig. 4; lane 6). The eluted fraction was then dialyzed against 2 L of dialysis buffer (2 mM Tris, and 5 mM NaCl, pH 7.0) to remove imidazole and was concentrated using a vacufuge. Protein concentration was determined using UV spectrophotometer (extinction coefficient 37,360 $M^{-1}cm^{-1}$). The yield of mCherry-Nt-RanBP9 was 30 mg/L. The fusion protein was then cleaved using thrombin (0.5 U/mg, 24 h at room temperature) to generate tag-free Nt-RanBP9. The sample from the thrombin cleavage reaction was then loaded into a RP-HPLC column and a differential gradient from 5% to 95% ACN was used to fractionate (Fig. 4c). With a shallow gradient between 40 and 55% ACN, a narrow fraction eluting at 31 min and a broad peak between fractions at 32 min and 36 min were observed (Fig. 4c). MALDI-ToF mass spectrometry analyses of the fractions revealed that the fraction corresponding to the 31 min contained Nt-RanBP9 with *m/z* value of 11989.1 kDa. However, we also observed significant number of low molecular-weight fragments which were neither resolved by HPLC nor by other purification techniques.

3.3.3. *mEGFP-Nt-RanBP9*

As described above, mCherry-Nt-RanBP9 could not be obtained in a pure form due to co-elution of proteolytic fragments. As mCherry tag is prone to get cleaved compared to GFP [14], final construct of Nt-RanBP9 was designed with a cleavable mEGFP tag on the *N*-terminus so that proteolytic degradation during expression and purification could be minimized. As in the case of mCherry-fusion, mEGFP-tagged Nt-RanBP9 also showed good level of expression with detectable green

color of cells, however, didn't show up in Coomassie blue staining (Fig. 3c). The protein was subjected to purification methods identical to that for mCherry-Nt-RanBP9. The protein was eluted with 400 mM imidazole (Fig. 5b; lane 6). The yield of the fusion protein was ~47 mg/L. The HPLC chromatogram of the thrombin-cleaved mEGFP-Nt-RanBP9 sample showed better resolved chromatogram than one obtained for mCherry-Nt-RanBP9 with Nt-RanBP9 eluting at 50% ACN as a narrow peak at 62 min (Fig. 5c). The yield of pure Nt-RanBP9 protein was approximately 8 mg/L of cell culture. SDS-PAGE analysis of this fraction revealed a single band corresponding to ~13 kDa (Fig. 5c; inset). The slightly altered migration of bands (MW 12 kDa) is often observed with intrinsically disordered proteins. MALDI-ToF analysis showed a pure protein with a m/z value of 12006.3 Da (Fig. 5d). Biophysical characterization of the purified protein using circular dichroism (CD) revealed a random coil signature with a minimum at 200 nm indicating a disordered structure for the protein as predicted by PONDR (Fig. 5e).

4. Conclusions

With the increasing significance of LCRs in biology, it is imperative to establish robust expression and purification methodologies to assist future advances in the field. The work presented here provides a modified cloning and purification method for the expression and characterization of the *N*-terminal LCR of RanBP9 protein called Nt-RanBP9, which has remained unknown for a long time. Perhaps the lack of existing information on Nt-RanBP9 could be linked to its difficulty of expression and purification. Therefore, the work presented here is a significant step in filling the knowledge-gap of understanding the role of multi-functional protein, RanBP9.

CRediT authorship contribution statement

Shailendra Dhakal: Data curation, Formal analysis, Investigation, Methodology, Writing - original draft, Writing - review & editing. **Krishna Sapkota:** Data curation, Formal analysis, Investigation, Methodology, Writing - review & editing. **Faqing Huang:** Conceptualization, Data curation, Writing - review & editing. **Vijayaraghavan Rangachari:** Conceptualization, Funding acquisition, Project administration, Resources, Writing - review & editing.

Acknowledgements

The authors would like to thank the following agencies for financial support: National Institute of Aging (1R56AG062292-01), National Institute of General Medical Sciences (R01GM120634), and the National Science Foundation (NSF CBET 1802793) to VR. The authors also thank the National Center for Research Resources (5P20RR01647-11) and the National Institute of General Medical Sciences (8 P20 GM103476-11) from the National Institutes of Health for funding through INBRE for the use of their core facilities. The authors thank Dr. Steven McKnight at UTSW for donating mCherry and EGFP plasmids.

References

[1] N. Radó-Trilla, M. Albà, Dissecting the role of low-complexity regions in the evolution of vertebrate proteins, BMC Evol. Biol. 12 (2012) 155.
[2] T.J. Nott, E. Petsalaki, P. Farber, D. Jervis, E. Fussner, A. Plochowietz, T.D. Craggs, D.P. Bazett-Jones, T. Pawson, J.D. Forman-Kay, Phase transition of a disordered nuage protein generates environmentally responsive membraneless organelles, Mol. Cell. 57 (2015) 936–947.
[3] A. Molliex, J. Temirov, J. Lee, M. Coughlin, A.P. Kanagaraj, H.J. Kim, T. Mittag, J.P. Taylor, Phase separation by low complexity domains promotes stress granule assembly and drives pathological fibrillization, Cell 163 (2015) 123–133.
[4] J.C. Wootton, S. Federhen, Analysis of compositionally biased regions in sequence databases, Method Enzymol266, 1996, pp. 554–571.
[5] L.M. Salemi, M.E. Maitland, C.J. McTavish, C. Schild-Poulter, Cell signalling pathway regulation by RanBPM: molecular insights and disease implications, Open biology 7 (2017) 170081.
[6] J.P. Palavicini, B.N. Lloyd, C.D. Hayes, E. Bianchi, D.E. Kang, K. Dawson-Scully, M.K. Lakshmana, RanBP9 plays a critical role in neonatal brain development in mice, PloS One 8 (2013).
[7] M.K. Lakshmana, J.Y. Chung, S. Wickramarachchi, E. Tak, E. Bianchi, E.H. Koo, D.E. Kang, A fragment of the scaffolding protein RanBP9 is increased in Alzheimer's disease brains and strongly potentiates amyloid-β peptide generation, Faseb. J. 24 (2010) 119–127.
[8] J.S. Bae, J.Y. Kim, B.L. Park, H.S. Cheong, J.H. Kim, S. Namgoong, J.O. Kim, C.S. Park, B.J. Kim, C.S. Lee, Investigating the potential genetic association between RANBP9 polymorphisms and the risk of schizophrenia, Mol. Med. Rep. 11 (2015) 2975–2980.
[9] J. Woo, A. Jung, M. Lakshmana, A. Bedrossian, Y. Lim, J. Bu, S. Park, E. Koo, I. Mook-Jung, D. Kang, Pivotal role of the RanBP9-cofilin pathway in A β-induced apoptosis and neurodegeneration, Cell Death Differ. 19 (2012) 1413–1423.
[10] E. Atabakhsh, J.H. Wang, X. Wang, D.E. Carter, C. Schild-Poulter, RanBPM expression regulates transcriptional pathways involved in development and tumorigenesis, Am. J. Cancer Res. 2 (2012) 549.
[11] K.W. Yoo, M. Thiruvarangan, Y.M. Jeong, M.S. Lee, S. Maddirevula, M. Rhee, Y.K. Bae, H.G. Kim, C.H. Kim, Mind bomb-binding partner RanBP9 plays a contributory role in retinal development, Mol 40 (2017) 271.
[12] L.M. Salemi, S.O. Loureiro, C. Schild-Poulter, Characterization of RanBPM molecular determinants that control its subcellular localization, PloS One 10 (2015).
[13] H. Nishitani, E. Hirose, Y. Uchimura, M. Nakamura, M. Umeda, K. Nishii, N. Mori, T. Nishimoto, Full-sized RanBPM cDNA encodes a protein possessing a long stretch of proline and glutamine within the N-terminal region, comprising a large protein complex, Gene 272 (2001) 25–33.
[14] M. Kato, S.L. McKnight, Cross-β polymerization of low complexity sequence domains, Methods 9 (2017) a023598.
[15] F. Huang, J.R. Spangler, A.Y. Huang, In vivo cloning of up to 16 kb plasmids in E. coli is as simple as PCR, PloS One 12 (2017) e0183974.
[16] P. Romero, Z. Obradovic, X. Li, E.C. Garner, C.J. Brown, A.K. Dunker, Sequence complexity of disordered protein, Proteins 42 (2001) 38–48.
[17] K. Peng, S. Vucetic, P. Radivojac, C.J. Brown, A.K. Dunker, Z. Obradovic, Optimizing long intrinsic disorder predictors with protein evolutionary information, J. Bioinf. Comput. Biol. 3 (2005) 35–60.
[18] K. Peng, P. Radivojac, S. Vucetic, A.K. Dunker, Z. Obradovic, Length-dependent prediction of protein intrinsic disorder, BMC Bioinf. 7 (2006) 208.
[19] P. Bubeck, M. Winkler, W. Bautsch, Rapid cloning by homologous recombination in vivo, Nucleic Acids Res. 21 (1993) 3601–3602.
[20] J.D. Oliner, K.W. Kinzler, B. Vogelstein, In vivo cloning of PCR products in E. coli, Nucleic Acids Res. 21 (1993) 5192–5197.
[21] C. Li, A. Wen, B. Shen, J. Lu, Y. Huang, Y. Chang, FastCloning: a highly simplified, purification-free, sequence- and ligation-independent PCR cloning method, BMC Biotechnol. 11 (2011) 92.
[22] P. Cao, L. Wang, G. Zhou, Y. Wang, Y. Chen, Rapid assembly of multiple DNA fragments through direct transformation of PCR products into E. coli and Lactobacillus, Plasmid 76 (2014) 40–46.
[23] A.P. Jacobus, J. Gross, Optimal cloning of PCR fragments by homologous recombination in Escherichia coli, PloS One 10 (2015) e0119221.
[24] M. Kostylev, A.E. Otwell, R.E. Richardson, Y. Suzuki, Cloning should Be simple: Escherichia coli DH5alpha-mediated assembly of multiple DNA fragments with Short end homologies, PloS One 10 (2015) e0137466.
[25] J. Garcia-Nafria, J.F. Watson, I.H. Greger, I.V.A. cloning, A single-tube universal cloning system exploiting bacterial in Vivo Assembly, Sci. Rep. 6 (2016) 27459.
[26] S. Contreras-Martos, H.H. Nguyen, P.N. Nguyen, N. Hristozova, M. Macossay-Castillo, D. Kovacs, A. Bekesi, J.S. Oemig, D. Maes, K. Pauwels, P. Tompa, P. Lebrun, Quantification of intrinsically disordered proteins: a problem not fully appreciated, Front. Mol. Biosci. 5 (2018).
[27] E. Rücker, G. Schneider, K. Steinhäuser, R. Löwer, J. Hauber, R.H. Stauber, Rapid evaluation and optimization of recombinant protein production using GFP tagging, Protein Expr. Purif. 21 (2001) 220–223.